Purification and Characterization of a Transmembrane Domain-Deleted Form of Lecithin Retinol Acyltransferase†

Dean Bok,‡,§,|| Alberto Ruiz,§ Orna Yaron,§ Wan Jin Jahng,⊥ Arghya Ray,⊥ Linlong Xue,⊥ and Robert R. Rando*,⊥

Department of Biological Chemistry and Molecular Pharmacology, Harvard Medical School, and Department of Neurobiology, Jules Stein Eye Institute, and Brain Research Institute, University of California, Los Angeles, California 90095

Received February 12, 2003

ABSTRACT: Lecithin retinol acyltransferase (LRAT) catalyzes the esterification of all-*trans*-retinol into all-*trans*-retinyl ester, an essential reaction in the vertebrate visual cycle. Since all-*trans*-retinyl esters are the substrates for the isomerization reaction that generates 11-*cis*-retinoids, this esterification reaction is essential in the operation of the visual cycle. In addition, LRAT is the founder member of a series of proteins, which are of novel sequence and have unknown functions. Native LRAT is an integral membrane protein and has never been purified. To obtain a pure LRAT, the N- and C-transmembrane termini were deleted and replaced with a poly His tag for the purpose of purification. This truncated form of LRAT, referred to as tLRAT, has been expressed in bacteria and fully purified. tLRAT is catalytically active and processes all-*trans*-retinol at least 10-fold more efficiently than 11-*cis*-retinol, the precursor to the visual chromophore. While tLRAT can be robustly expressed in bacteria, it requires detergent for extraction, as the enzyme still contains hydrophobic domains, which may interact. Indeed, tLRAT can oligomerize and forms dimers. Native LRAT also forms functional homodimers. These studies pave the way for the preparation of large-scale amounts of pure tLRAT for further mechanistic and structural studies.

Lecithin retinol acyltransferase (LRAT)[1] is a transmembrane protein that forms retinyl esters in a variety of tissues (*1*−*4*). In some cells, retinyl esters are thought to be a storage form of all-*trans*-retinol (Vitamin A). These esters are hydrolyzed by retinyl ester esterases when there is a need for conversion of retinol to one or another of its retinoid derivatives, such as retinoic acid (*5*). In the context of the retinal pigment epithelium (RPE) of the eye, however, the retinyl esters, primarily retinyl palmitate, serve not only as a reservoir but are also the substrate for an isomerohydrolase (*6*, *7*). This enzyme utilizes the energy stored in the retinyl ester bond to produce 11-*cis*-retinol, the penultimate retinoid in the production of 11-*cis*-retinaldehyde, the chromophore for the retinal photoreceptor photopigments (*7*−*10*).

The purification of native, membrane-bound LRAT has not been achieved; nevertheless, a substantial amount is known about this enzyme. Early studies demonstrated that it is extremely sensitive to thiol-directed reagents, such as organomercurials, but relatively insensitive to other group specific reagents, suggesting that LRAT might be a thiol enzyme mechanistically (*5*, *11*, *12*). Kinetic analysis on LRAT revealed an ordered ping-pong bi-bi mechanism (*13*). In this mechanism, lecithin binds first and transfers an acyl group to an active-site nucleophile, followed by the binding of vitamin A and the transfer of the acyl group to the latter, generating a retinyl ester (*13*). LRAT is readily and specifically inactivated in an affinity-labeling mode by all-*trans*-retinyl bromoacetate (*14*), enabling the identification and eventual cloning of the enzyme (*4*). Site directed mutagenesis and kinetic analysis of full-length LRAT expressed autologously in HEK cells allowed further insights to be drawn concerning LRAT function (*4*). Two cysteine residues important for catalysis (C161 and C168) have been identified (*15*). It is reasonable to suggest that one of the cysteine residues (probably C161) is the active-site nucleophile of LRAT, which accepts an acyl group from lecithin (*15*). In addition, two histidine residues are also essential for LRAT activity (*16*).

The full-length sequence of LRAT shows that it is unrelated to any proteins of known function (*4*, *14*). LRAT is, however, the founder member of a family of proteins of unknown function (*4*, *17*, *18*). These proteins are functionally diverse and include tumor suppressors (*4*, *17*) and putative

† The work described here was supported by NIH Grant EY-04096 (to R.R.R.) and by NIH Grants EY-00444, EY-00331, and the Dolly Green Endowed Chair (to D.B.).

* To whom correspondence should be addressed. Tel.: (617) 432-1794. Fax: (617) 432-0471. E-mail: robert_rando@hms.harvard.edu.

‡ Department of Neurobiology, University of California−Los Angeles.

§ Jules Stein Eye Institute, University of California−Los Angeles.

|| Brain Research Institute, University of California−Los Angeles.

⊥ Harvard Medical School.

[1] Abbreviations: AEBSF, 4-(2-aminoethyl)benzenesulfonyl fluoride; BCA, biconcinic acid; BME, β-mercaptoethanol; BSA, bovine serum albumin; CHAPS, 3-[(3-chloroamidopropyl)dimethylammonio]-1-propane sulfonate; CHAPSO, 3-[(3-chloroamidopropyl)dimethylammonio]-2-hydroxy-1-propanesulfonate; DMF, dimethyl formamide; DMSO, dimethyl sulfoxide; DPPC, α-dipalmitoyl phosphatidyl choline; DTT, dithiothreitol; ECL, enhanced chemiluminescence; EDTA, ethylenediamine tetraacetic acid; E-64, *trans*-epoxysuccinyl-L-leucylamido-(4-guanidino)butane; hLRAT, human lecithin retinol acyltransferase; IPTG, isopropylthiogalactoside; PBS, phosphate-buffered saline; RPE, retinal pigment epithelium; SDS−PAGE, sodium dodecyl sulfate polyacrylamide gel electrophoresis; THF, tetrahydrofuran; tLRAT, truncated lecithin retinol acyltransferase.

10.1021/bi0342416 CCC: $25.00 © 2003 American Chemical Society
Published on Web 05/02/2003

viral proteases (*18*). All of these proteins contain conserved histidine and cysteine residues that are probably part of a catalytic diad or triad (*18*). Further experiments will be required to elucidate the precise functions of these novel proteins.

Since full-length LRAT has never been studied in its purified form, the full characterization of this apparently unique enzyme has not been achieved. Purified LRAT would enable a full delineation of its structure and mechanism of action, as well as enabling the preparation of specific antibodies for histochemical and other uses. Unfortunately, the full-length protein contains at least two transmembrane domains at its N- and C-termini, which confound purification (*4*). Expression of this protein in mammalian HEK cells has been successful, but only very limited quantities of protein can be extracted (*4*). Moreover, LRAT expressed in HEK cells is, as expected, not readily purified, so that while mutational studies are possible, the enzyme cannot be used for structural investigations or used for the preparation of monoclonal and polyclonal antibodies. Repeated attempts at expressing full length LRAT in bacteria also have not met with success. To prepare a purified form of LRAT that could be produced in large quantities, we sought to engineer a His-tagged and deleted transmembrane domain form of catalytically active LRAT, which can be expressed in bulk in bacteria.

A method for the preparation of a truncated histidine-tagged form of LRAT (tLRAT) in which the primary sequence extends from residue 31−196, thereby deleting the putative transmembrane domains, is reported here (*4*). None of the residues known to be required for catalysis are found in these domains, leading to the expectation that tLRAT ought to be active. This expectation is realized.

Although tLRAT is not fully soluble without the aid of detergents, possibly as a consequence of strong protein−protein interactions, it can be readily purified in milligram quantities when extracted with 1% sodium dodecyl sulfate (SDS) as shown here. While tLRAT activity is insignificant in 1% SDS, it recovers substantial enzymatic activity in low concentrations of SDS (0.05%). tLRAT can also be extracted in reduced quantities with other, milder detergents such as Triton X-100, octyl-D-glucopyranoside, CHAPS, and CHAPSO. Among these, CHAPSO provides the highest yield and the lowest level of misfolded protein as judged by NMR. CHAPSO-extracted and purified tLRAT should be suitable for mechanistic and structural studies utilizing nuclear magnetic resonance (NMR), X-ray diffraction, and site-directed spin labeling methods.

EXPERIMENTAL PROCEDURES

Materials. The expression vector, pET 21b(+) was obtained from Novagen, Inc. (Madison, WI), and the polymerase chain reaction (PCR) core reagent was from Applied Biosystems (Foster City, CA). *Escherichia coli* One Shot cells, BL21 STAR (DE3) cells, and ProBond Resin for purification of histidine-tagged (6X His-tag) and Precast gels (4−20%, 8 × 8 cm) for SDS/native polyacrylamide gel electrophoresis (PAGE) were from Invitrogen (Carlsbad, CA). The Wizard Plus Miniprep system was from Promega Corp. (Madison, WI). Sequenase 2.0 for dideoxy chain termination sequence analysis was obtained from USB Corp. (Cleveland, OH). Centricon Centriprep concentrators were from Amicon (Beverly, MA). [11,12-^{3}H,^{3}H-All-*trans*-retinol (49.7 Ci/mmol) was obtained from NEN Life Sciences (Boston, MA). Radioactive sodium borohydride [NaB^3H_4] was from NEN. 11-*cis*-retinal was obtained from the National Eye Institute. Protease inhibitor cocktail (AEBSF, aprotinin, bestatin, EDTA, E-64, leupeptin, pepstatin A), L-α-dipalmitoylphosphatidylcholine (DPPC), bovine serum albumin (BSA), dithiothreitol (DTT) Laemmli buffer (*16*), Triton X-100 (TX-100), and Dalton VI molecular weight markers were from Sigma (St. Louis, MO). Benchmark prestained markers were from GibcoBRL Life Technologies (Grand Island, NY). The BCA protein determination kit, CHAPSO (3[(3-cholamidopropyl)-dimethylammonio]-2-hydroxy-1-propane sulfonate), Tween-80, Western blot blocking buffer, Gel-code Blue solution for Coomassie staining, and avidin−biotin complex (ABC) staining kit were purchased from Pierce (Rockford, IL). Avidin conjugated horseradish peroxidase for biotin detection and Precision Plus Protein Standards were from Bio-Rad (Hercules, CA). High performance liquid chromatography (HPLC) solvents were obtained from J. T. Baker (Phillipsburg, NJ). Sodium dodecyl sulfate (SDS), polyvinylidene fluoride membranes, the enhanced chemiluminescence (ECL) Western blotting and silver staining kit, and cyanogen bromide-activated Sepharose 4B were from Amersham Pharmacia Biotech (Piscataway, NJ). All other reagents were of analytical grade.

Preparation of LRAT/pET Expression Vectors. The hLRAT protein is a polypeptide of 230 amino acid residues with a calculated molecular mass of 25.3 kDa. This protein contains at least two transmembrane domains at positions 9−31 at the amino terminal and at positions 196−222 at the carboxy terminal (*15*, *20*). Attempts were made at generating full-length and truncated constructs of this protein. For the generation of the tLRAT construct, residues from both ends of the protein at positions 1−30 of the amino terminus and 197−230 from the carboxy terminus, respectively, were deleted by standard recombinant DNA methods. PCR technology was used for the generation of the full-length and truncated constructs, and hRPE cDNA clones previously published (*4*) were used as DNA templates for PCR amplifications. A PCR core reagent set was obtained from Applied Biosystems and used according to the provider's instructions. DNA amplification was performed in a Robocycler 40 apparatus (Stratagene, La Jolla, CA). For the generation of the construct encoding the entire LRAT protein, the following set of oligonucleotide primers was used: forward, 5′CATATGAAGAACCCCATGCTGGAGGTG3′ and reverse, 5′CTCGAGGCCAGCCATCCATAGGAAGAA3′.

For the purpose of unidirectional cloning, additional Nde I and Xho I restriction sites were attached to the 5′ end of each primer. The pET 21b(+) vector was then linearized with NdeI and Xho I and subsequently ligated with the gel purified PCR product using the same cohesive ends. Utilizing the same strategy, a truncated LRAT (tLRAT) was created with the following set of primers: forward, 5′CATATGGGCGAAGACAAAGGGAGGAACAGT3′ and reverse, 5′CTCGAGAACACTTCTCTGATCACGAATAAT3′. An initiation of translation site (ATG) was added at the amino terminus, which includes an Nde I restriction site, and an extra amino acid residue Glu was added at the carboxy terminus by virtue of an Xho I restriction site. A His-tag of

six Histidines was also incorporated at this end for the purpose of protein purification, thus generating a truncated LRAT (tLRAT) protein of 173 amino acid residues with a calculated molecular mass of 19.9 kDa. After amplification of the contructs in *E. coli* One Shot cells, plasmid DNA was extracted using the Wizard plus miniprep system and evaluated by 2% agarose gel electrophoresis. Sequence analysis using the dideoxy chain termination method (Sequenase 2.0) was performed on each construct to confirm the presence, orientation, and correct nucleotide sequence of each DNA insert.

Expression of tLRAT in Bacteria. Plasmid DNA was introduced into the BL 21 STAR (DE3) strain of *E. coli* by standard methods (*21*). The cells were grown in Luria-Bertani (LB) medium in 1 L batches at 30 °C for 6 h following induction with IPTG at a final concentration of 0.5 mM. Cells were pelleted by centrifugation at 8000*g* for 10 min, and the pellet was washed with fresh LB medium. The bacteria were disrupted at 37 °C for 15 min with lysis buffer (50 mM Tris, pH 8.0; 100 mM NaCl) containing 100 μg/mL of lysozyme. EDTA was omitted from the lysis buffer because it is incompatible with Ni column affinity purification. The lysate was sonicated by 10, 10-s bursts with a Microson Ultrasonic Cell Disrupter (Heat Systems Ultrasonics, Inc.) set at 50% output power and centrifuged at 30 000*g* for 20 min. The tLRAT partitioned into the insoluble fraction.

Solubilization and Affinity Purification of Histidine-Tagged tLRAT for Antibody Production. Because of previous experiences suggesting that LRAT activity is labile in the absence of DTT (*2*), we initially carried out the purification steps under an argon atmosphere since DTT, the reducing agent used in our previous studies, interferes with the performance of Ni affinity purification (*4*). This was achieved by using a plastic glovebag (Instruments for Research and Industry, Model X-27-27) attached to an Argon source to produce an inflatable chamber in which the affinity column could be manipulated.

Truncated LRAT was extracted from the resuspended membrane pellet in buffered 1% SDS (20 mM sodium phosphate, 500 mM NaCl, pH 7.8) at 20 °C. The sample was centrifuged at 30 000*g* at 20 °C for 20 min, and the supernatant containing the solubilized tLRAT was collected. The pellet was resuspended in 1% SDS in extraction buffer for an additional hour and centrifuged again, and the second supernatant was added to the first. ProBond Resin for the purification of 6X His-Tagged proteins (Ni column) was poured into a 10 mL column. Before loading of the tLRAT sample, the SDS concentration was reduced to 0.25% to prevent interference by SDS with the protein/resin binding. The Ni column was equilibrated with 0.25% SDS in the extraction buffer. After the sample was loaded, the column was washed with phosphate buffer in three steps from the starting pH of 7.8 to 6.0, 5.3, and 4.0. The volume of each elution buffer was in the proportion recommended by the vendor (32 mL). Most of the tLRAT eluted at pH 6.0 and 5.3, with a minor amount eluting at pH 4.0. Following elution, DTT was added to each fraction to a final concentration of 2 mM, and argon was omitted from the protocol thereafter. tLRAT remained in solution at 20 °C in 0.1% SDS but precipitated at lower temperatures (4 °C) and lower detergent concentration ($<$0.05% SDS). The samples could be returned to solution by heating at 37 °C. The protein was concentrated with a Centriplus YM-10 filter concentrator (Amicon) while centrifuging at 2400*g* at 20 °C. The final yield of tLRAT from 1 L of cultured cells ranged from 1 to 2 mg. Subsequent analysis of tLRAT purified under ambient conditions revealed that it maintained activity in the absence of Argon so this precaution was omitted.

Alternatively, solubilized tLRAT could be purified by Ni column affinity chromatography using an imidazole buffer step gradient elution. The sample was loaded on a Ni column preequilibrated with the washing buffer (20 mM sodium phosphate, pH 7.4, 500 mM NaCl, 10 mM imidazole). tLRAT was purified by stepwise gradient elution (20 mM sodium phosphate buffer, pH 7.4, 500 mM NaCl, imidazole concentration: 10, 20, 40, 60, 100, 300, 500 mM). The enzyme was found mostly in fractions between 300 and 500 mM imidazole concentration. tLRAT fractions were collected and concentrated by centrifugal filtration (8160*g*, 5 kDa cut, UFV5BCC00, 5k NMWL membrane, Millipore). Concentrated tLRAT was dialyzed under reducing conditions (0.1% Triton X-100, 1 mM DTT, sodium phosphate 50 mM, pH 7.5). Purified tLRAT was analyzed by SDS−PAGE, Western blots, activity assays, and mass spectrometry.

Generation of tLRAT Antibodies. tLRAT expressed in *E. coli BL-21 Star DE3* cells was purified to homogeneity by Ni column chromatography. The purity of tLRAT was assessed by PAGE and silver staining and was shown to be free of contaminating proteins within the level of sensitivity of this method. The authenticity of the purified protein was verified by Western blot analysis, using anti LRAT peptide antibodies characterized previously (*4*). Two rabbits were repetitively immunized with tLRAT emulsified in complete Freund's adjuvant following a standard protocol. The Polyclonal antiserum was generated by contract with Alpha Diagnostics International (San Antonio, TX). Titers were monitored by ELISA prior to utilization for immunocytochemistry and Western blot analysis. Affinity-purified antibodies were prepared for Western blotting and immunocytochemistry by coupling purified tLRAT to cyanogen bromide-activated Sepharose 4B according to the vendor's instructions.

Western Blot Analysis. Polyclonal anti-LRAT antibody formation was reported previously (*4*). After protein separation by SDS−PAGE, proteins were transferred to polyvinylidene fluoride (PVDF) membranes using transfer buffer (Tris 25 mM, glycine 192 mM, ethanol 20%) and a semidry transfer apparatus. The membrane was blocked with 5% nonfat dried milk for 2 h at room temperature. Anti-LRAT antibody (1:4000 dilution), anti-rabbit Ig linked horseradish peroxidase (1:8000 dilution) from donkey, and the enhanced chemiluminescence (ECL) system were used to detect tLRAT band.

Solubilization and Activity Assay of tLRAT. tLRAT solubility was tested using 1% SDS, Triton X-100, CHAPSO, Tween-80, and DMSO. The procedure involved incubation of the cell pellet for 2 h in an ice-cold 0.1 M Tris-HCl buffer containing a protease inhibitor cocktail (AEBSF, aprotinin, bestatin, EDTA, E-64, leupeptin, pepstatin A) at pH 8.3. All incubations were performed at 4 °C. After 2 h, the cell suspension was equally distributed in different tubes. Detergents were added to respective tubes to make a final concentration of 1% detergent. A cell suspension absent detergent was used as a control. Cells were sonicated on ice

using a Branson Sonifier 250 containing a needle probe by applying 10 mild bursts, each for 30 s, with an interval of 30 s between consecutive bursts. Cell lysates containing detergents were placed on a rocker and incubated at 4 °C overnight. Finally, the suspension mixtures were centrifuged at 13 800 or 265 000*g* for 30 min at 4 °C. The supernatant containing tLRAT was collected and used for further analysis. The pellet thus obtained was also redissolved in the same buffer and tested for tLRAT activity. Kinetic activity measurements and the synthesis of ^{3}H-11-*cis*-retinol are described in the Supporting Information.

Analysis of tLRAT Oligomerization. tLRAT oligomerization was tested under nonreducing condition by PAGE and Western blotting. Nondenaturing sample buffer (without DTT and SDS, Tris-HCl 312.5 mM, 50% glycerol, 0.05% bromophenol blue, pH 6.80) was used to reveal tLRAT oligomer formation as compared to DTT (5 mM) and/or SDS (2%) control with and without heating. Running buffer contained Tris base (192 mM, final pH 8.3), glycine (192 mM), and SDS (0.1%). Mass spectrometric measurements are described in the Supporting Information.

Immunocytochemistry of Bovine Retina and Liver. Formaldehyde was prepared from paraformaldehyde according to standard methods. Fresh bovine eyes and liver were obtained from a local slaughterhouse immediately after excision from the animal, and the tissues were fixed by immersion on site. Following removal of the cornea, iris, lens, and vitreous body, the remaining posterior portion of the eye and small pieces of liver were fixed for 24 h in a 0.1 M sodium phosphate-buffered, 4% formaldehyde solution (pH 7.2). Following fixation, strips of the choroidal layer with attached retina were dissected from the scleral layer of the eye. The choroid/retina was dehydrated in a graded ethanol series (50−100%) and embedded in paraffin. During this step, the neurosensory retina detached from the choroid/retinal pigment epithelium.

Immunocytochemistry was performed at 21 °C in a humidified chamber. The deparaffinized sections were treated for 20 min with PBS buffered 0.3% hydrogen peroxide and then exposed to affinity purified antibodies at a concentration of 0.01 $A_{280\ nm} = 1$ A units. Preimmune control sections were treated alongside the experimental sections. Primary antibody binding was visualized with the avidin−biotin enzyme complex (ABC) technique according to instructions provided by the vendor. Experimental and control sections were imaged with a 40× planapochromatic oil immersion lens and a Zeiss Axiovert microscope fitted with a CoolSNAP digital camera (Diagnostic Instruments, Sterling Heights, MI) and Imago Pro Software (Media Cybernetics, Silver Springs, MD). Images were rendered in Adobe Photoshop (Adobe Systems Incorporated).

RESULTS

Cloning, Expression, and Purification of tLRAT. Multiple attempts at expression of full-length LRAT in bacteria have, unfortunately, not met with success. A series of attempts at expression did not provide evidence of protein expression, either by silver gel SDS−PAGE or by Western blot detection. This led to an interest in expressing a more soluble form of enzymatically active LRAT. A truncated form of LRAT (tLRAT), lacking the transmembrane N- and C-termini, was designed and expressed in bacteria. Induction of tLRAT expression in *E. coli* by IPTG was robust. The induced protein was readily visible on silver-stained gels of bacterial lysates (Figure 1). Although lacking its putative transmembrane domains, tLRAT remained insoluble in the absence of detergents. SDS was the most effective detergent for extraction (see details below) so purification for the purpose of antibody production was carried out in 1% SDS. When applied to a Ni column and eluted with a pH step gradient, the protein eluted at pH 6.0 and 5.3 rather than pH 4.0, which is more typical for proteins purified by this method. Virtually no protein was eluted at pH 4.0 (Figure 1). Eluted tLRAT fractions were pooled, and the amount of protein harvested was quantified by the BCA method. The yield of protein was 1−2 mg/L of cultured bacteria.

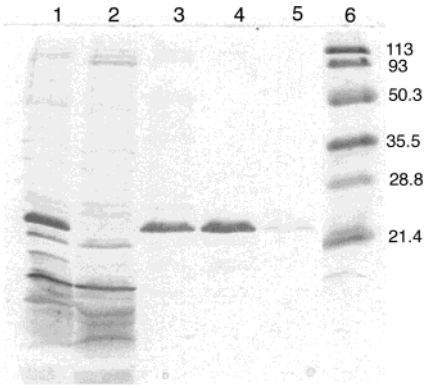

FIGURE 1: Silver stained SDS−PAGE of tLRAT purified on Ni column in SDS. Lane 1, cell extract; lane 2, Ni column flowthrough; lane 3, pH 6.0 elution; lane 4, pH 5.3 elution; lane 5, pH 4.0 elution; and lane 6, molecular weight markers.

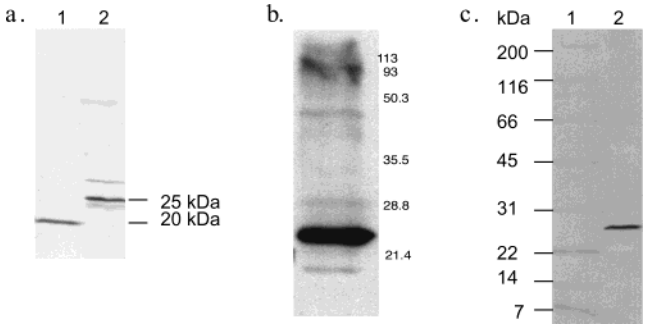

FIGURE 2: (a) Western blot of the purified tLRAT (lane 1) and LRAT (lane 2) from the crude RPE. The membrane was probed with anti-LRAT peptide polyclonal antibody (1:4000), anti-rabbit Ig linked horseradish peroxidase (1:8000), and ECL reagent. (b) Western blot of tLRAT of a bacterial lysate reacted with anti-LRAT protein antibody. (c) Western blot of LRAT in the RPE (lane 2). Molecular weight markers (lane 1) are 200, 116, 66, 45, 31, 22, 14, and 7 kDa, respectively.

Generation of Polyclonal Antibodies Against tLRAT. A Western blot of the purified tLRAT and the crude LRAT from the RPE detected with the anti-LRAT peptide antibodies is shown in Figure 2a (*4*). Specific staining of a ∼20 kDa protein band for tLRAT and 25 kDa band for LRAT from crude RPE are evident. Furthermore, purified tLRAT was used for the immunization of two rabbits, both of which produced antibodies. A Western blot of a tLRAT from a precolumn bacterial lysate and the native LRAT in the RPE reacted with the resulting polyclonal anti-LRAT antibody is shown in Figure 2b,c.

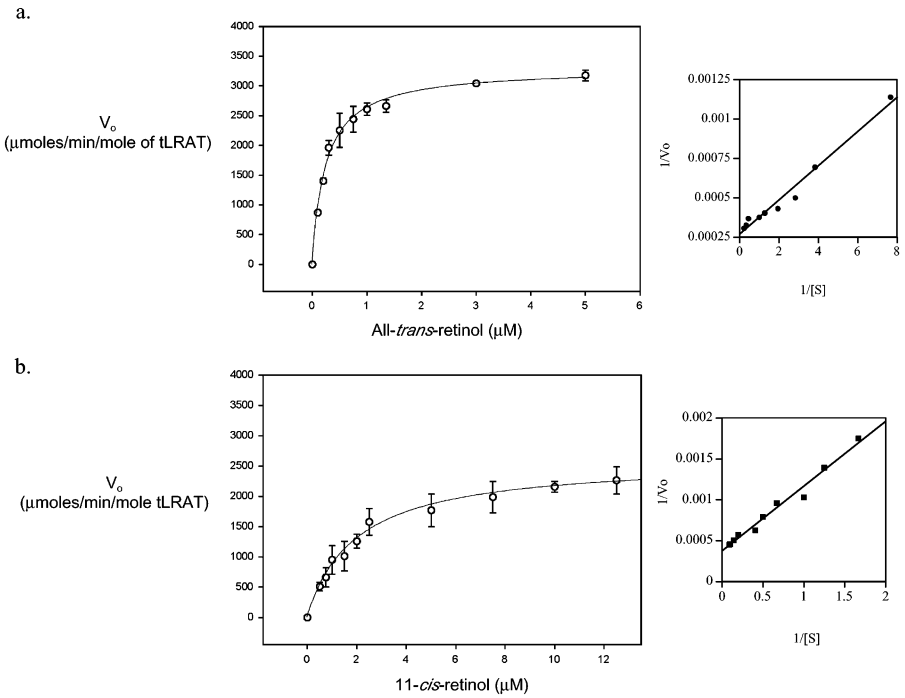

FIGURE 3: Steady-state kinetics of tLRAT using all-*trans*-retinol and 11-*cis*-retinol as substrates. Esterification activity of tLRAT was monitored by following the formation of retinyl esters using tritium labeled all-*trans*-retinol and 11-*cis*-retinol along with DPPC. 5−10 μg of purified tLRAT was used in 100 mM Tris-HCl (100 μL) at pH 8.3 containing 220 μM DPPC, 0.6% BSA, 1 mM EDTA, 2 mM DTT, 0.1% CHAPSO, and 0.2 μM of the retinol. (a) The initial velocity of all-*trans*-retinyl ester formation reaction and subsequent Lineweaver−Burk plot. (b) The initial velocity of 11-*cis*-retinyl ester formation reaction and subsequent Lineweaver−Burk plot.

Kinetics of Purified tLRAT. Purification of histidine tagged tLRAT using a Ni column in 1% SDS provided pure tLRAT as judged by silver stained SDS−PAGE (Figure 1). However, the activity assay and a preliminary NMR study of the protein extracted using this method showed both little enzymatic activity and possibly an unfolded structure. However, 1:20 dilution of samples purified in 1% SDS (final concentration of 0.05% SDS) followed by consecutive dialysis against 1% DTT and 1% EDTA showed substantial recovery of activity. Kinetic studies were performed on tLRAT samples prepared in this way.

The primary goal of the kinetic study was to establish activity of tLRAT prepared and purified as indicated above (extracted in 1% SDS-final SDS, 0.05% for kinetics)(Figure 3). This study was performed by steady-state kinetic analysis monitoring retinyl ester formation from retinol in the presence of saturating levels of DPPC. The time-course of retinyl ester formation by tLRAT is presented in Figure 3a,b. The purified tLRAT retains its activity and provides V_{max} and K_m values, as well, of course, as the second-order rate constant V_{max}/K_m. tLRAT, prepared and purified as indicated above, had a $V_{max} = 0.17 \pm 0.003$ nmol/min/mg and a $K_m = 0.24 \pm 0.03$ μM for the all-*trans*-retinol to all-*trans*-retinyl palmitate conversion (Figure 3a). As RPE membranes also produce 11-*cis*-retinyl esters (*2*, *3*), it was important to determine whether pure tLRAT is capable of using 11-*cis*-retinol as substrate. It is certainly possible that a second enzyme in RPE membranes is responsible for esterifying 11-*cis*-retinol. For the 11-*cis*-retinol to 11-*cis*-retinyl ester formation reaction, the $V_{max} = 0.13 \pm 0.004$ nmol/min/mg and the $K_m = 2.08 \pm 0.04$ μM were obtained (Figure 3b). These results show that tLRAT processes 11-*cis*-retinol but substantially less efficiently than with all-*trans*-retinol. The approximately 10-fold higher catalytic efficiency (V_{max}/K_m) of tLRAT for all-*trans*-retinol over 11-*cis*-retinol clearly indicates that 11-*cis*-retinol is a much weaker substrate for tLRAT than its all-trans isomer. Preference for all-*trans*-retinol as substrate was also observed in the kinetic analysis of full-length LRAT cloned and expressed in HEK 293 cells (*4*). Here, the V_{max}/K_m is about 20, with all-*trans*-retinol again being strongly favored as a substrate.

Extraction of tLRAT by Various Detergents. As mentioned above, tLRAT requires detergent for significant extraction from bacteria. Detergent extraction is critical for expressing maximal tLRAT activity. In the absence of added detergent, some tLRAT activity (approximately 20%) is present in the 13 800*g* supernatant while at 265 000*g* (<1% activity) is extracted. Since all of the tLRAT activity can be sedimented at higher speeds, it is unlikely that any fraction of tLRAT is truly soluble. Since tLRAT extracted in 1% SDS is inert, extraction methods were sought that directly yield active enzyme. Simple extractions methods, such as using guanidinium hydrochloride and urea were approximately as effective as 1% SDS but again yielded tLRAT with very minimal activity. Experiments were then performed to examine the relationship between the nature of the detergent used for extraction of tLRAT and its efficiency, both with respect to extent of extraction and the resultant tLRAT catalytic activity. tLRAT solubilization was examined by SDS−PAGE/Western blot analysis. Enzymatic activity measurements were performed on the tLRAT samples solubilized by the various detergents (Figure 4). In this figure, the data are normalized to 100% extraction for 1% SDS (Figure 4a) and 100% enzymatic activity for the extraction with CHAPSO (Figure 4b). As measured by densitometric analysis of the Western blots, 1% SDS extracts virtually all (>95%) of the tLRAT from bacteria, while CHAPSO extraction produces the highest overall enzymatic activity.

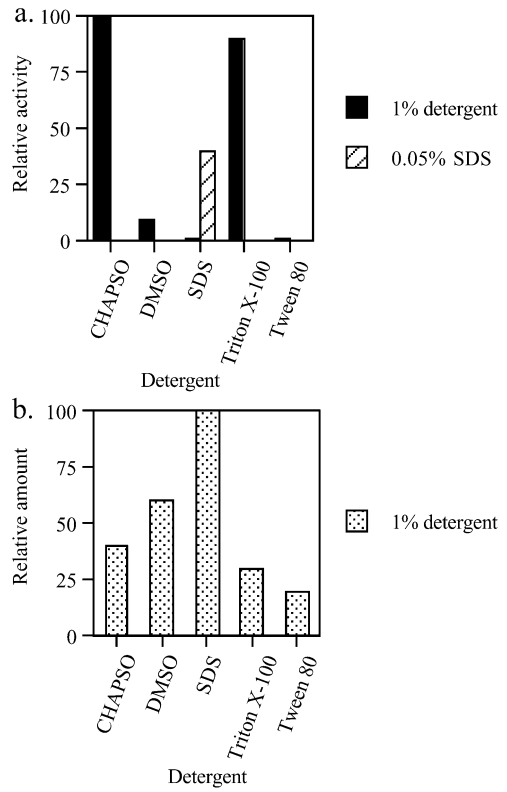

FIGURE 4: Relative activity and solibilization of tLRAT in the presence of different agents. (a) tLRAT was extracted with each detergent for 2−4 h at 4 °C, and all-*trans*-retinol esterification activity was measured as described in the Experimental Procedures. Relative amounts of tLRAT extracted were determined by SDS−PAGE/Western blot. In the absence of added detergent, minimum tLRAT activity (20%) was observed in the 13 800*g* centrifuged supernatant, while no activity (<1%) was observed in the 265 000*g* sample. (b) The relative extraction amounts and the catalytic activities showed about 10% variation depending on the mechanical force used (e.g., magnetic stirring vs gentle shaking). The values are the averages of at least five determinations.

As seen in Figure 4b, CHAPSO and Triton X-100 allowed for higher enzymatic activity than achieved with other detergents such as Tween 80 (<10%), DMSO (<10%), and SDS (<1%). This relative initial rate data, however, must be compared to the extraction efficiency of the different detergents. The extent of tLRAT extraction in different detergents varied from almost quantitative in the case of SDS, followed by DMSO (60%), CHAPSO (40%), and Triton X-100 (30%) (Figure 4a).

Dimer Formation of Purified tLRAT. PAGE Analysis. Native bovine LRAT showed functional homodimerization in RPE membranes based on nondenaturing PAGE and cross-linking studies coupled with kinetic analysis (*22*). It was of some interest to determine whether dimer formation would also occur with tLRAT, inasmuch as this latter enzyme is devoid of its putative N- and C-terminal transmembrane segments. To evaluate possible protein−protein interactions, which might stabilize oligomerization of tLRAT, several approaches were used. These include PAGE under different conditions, mass spectrometric analysis, and sedimentation equilibrium studies.

Under standard SDS−PAGE denaturing conditions, tLRAT migrates as a monomer (20 kDa) along with a small amount of dimer (40 kDa) (Figure 5). The absence of thiol reducing reagent enhances the amount of 40 kDa migrating

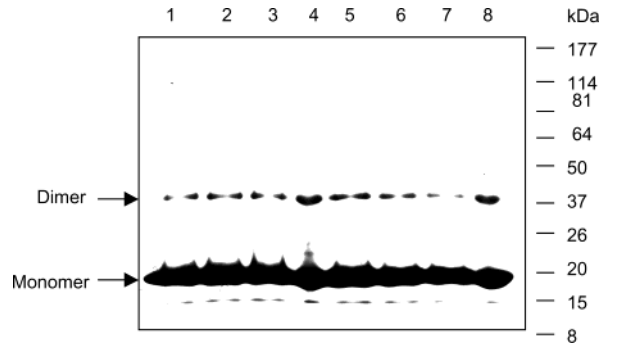

FIGURE 5: tLRAT homodimer analysis by mass spectrometry. Proteins were visualized by Coomassie blue staining after SDS−PAGE. His_{x6} tagged truncated LRAT (tLRAT) purified by Ni^{2+} column using an imidazole gradient elution buffer (10−500 mM). SDS−PAGE gel, in each lane, 40 μL (80 μg) of sample was loaded. Lanes 1−3 and 5−7, tLRAT in SDS (2%) + DTT (5 mM) + heating; lanes 4 and 8, tLRAT in SDS (2%) without DTT/heating. The 20 and 40 kDa bands were excised, trypsin digested, and analyzed by electrospray tandem mass spectrometry showing 13 (20 kDa) and 11 (40 kDa) LRAT peptides, respectively.

dimer band (Figure 5). Mass spectrometric investigation of this dimer shows only LRAT peptides, as shown in Table 1. From this result, it is concluded that tLRAT can form homodimers. Under nondenaturing conditions, by Western blotting analysis, tLRAT forms dimers, trimers, tetramers, and pentamers (Figure 6). MALDI-TOF mass spectrometry analysis supports this result revealing monomer (20 086 av. mass), dimer (40 094), trimer (60 196), and tetramer (80 697) peaks.

Ultracentrifugation Analysis. Sedimentation equilibrium studies of purified tLRAT were performed to examine oligomerization because of the protein−protein hydrophobic interactions under a standard set of nondenaturing conditions in solution. Once equilibrium between monomer and oligomers had been reached, absorption spectra at 280 nm were collected and analyzed based on global fitting to nonlinear least-squares analysis of monomer−dimer equilibrium model (*23*, *24*). The residuals (*y* axis, upper panel, Figure 7) represent Δ absorbance at 280 nm. The raw data (circles) and the global fit of an ideal monomer−dimer model (lines) are shown in the lower panel of Figure 7. It was determined that solubilized, purified tLRAT exists as a mixture of monomer and dimer. Higher order oligomers did not appear under these conditions.

Immunocytochemistry of Bovine Retina and Liver. To test the specificity of polyclonal antibodies against purified human tLRAT, we chose bovine retina and liver. Bovine tissue was selected both because of its availability and because a central region of the bovine retinal pigment epithelium overlying the reflective tapetum lacks melanin. Thus, the brown reaction product produced during color reaction following antibody binding cannot be confused with the brown color of melanin. The RPE was the only cell class in the retina that was specifically stained (Figure 8a). The nucleoplasm of the RPE was negative, consistent with the fact that tLRAT is an integral membrane protein, most likely localized to the smooth endoplasmic reticulum, which exists in abundance in the RPE.

Hepatocytes of the bovine liver were also specifically stained (Figure 8b). As in the RPE, staining was distributed throughout the cytoplasm but was absent from the nuclei.

Table 1: ESI MS/MS Analysis of tLRAT (20 kDa) and tLRAT Homodimer (40 kDa)

	20 kDa band	40 kDa band
MH^+	sequence	sequence
855.1520		LILGVIVK
885.0079	GDVLEVPR	GDVLEVPR
1011.3395		RLILGVIVK
1015.1545	ALLNEEVAR	ALLNEEVAR
1143.3286	KALLNEEVAR	KALLNEEVAR
1193.2987	YGTPISPQSDK	YGTPISPQSDK
1218.4539	ILLALTDDMGR	
1375.4399	NSFYETSSFHR	NSFYETSSFHR
1409.6255	ILVNHLDESLQK	
1588.6796	GRNSFYETSSFHR	
1660.8295	THLTHYGIYLGDNR	THLTHYGIYLGDNR
1901.1414	YGTPISPQSDKFCETVK	YGTPISPQSDKFCETVK
2000.3970	VAHMMPDILLALTDDMGR	
2241.4248	NSFYETSSFHRGDVLEVPR	NSFYETSSFHRGDVLEVPR
2691.9541	VDTVEDFAYGANILVNHLDESLQK	VDTVEDFAYGANILVNHLDESLQK
coverage	53%	48%

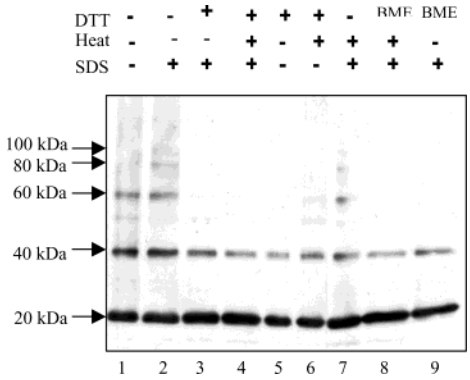

FIGURE 6: Purified tLRAT oligomer formation. Purified tLRAT was incubated 45 min in the reducing condition (DTT) and/or detergent (SDS). Protein was visualized by Western blot analysis. Lane 1, native sample buffer only; lane 2, SDS (2%); lane 3, SDS (2%) + DTT(10 mM); lane 4, SDS (2%) + DTT (5 mM) + heating; lane 5, DTT (5 mM); lane 6, DTT (5 mM) + heating (2 min); lane 7, SDS (2%) + heating (2 min); lane 8, SDS (2%) + BME (10%) + heating (2 min); and lane 9, SDS (2%) + BME (10%).

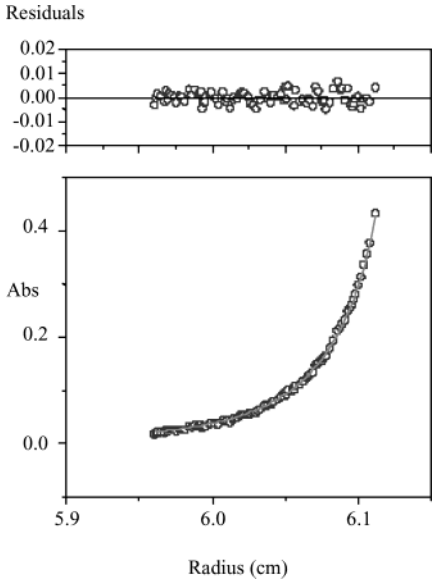

FIGURE 7: Sedimentation equilibrium analysis of tLRAT. tLRAT interaction analysis was performed in a Beckman Optima XL-A analytical ultracentrifuge using a 4-hole rotor and six channel cell. A solution of 100 μL of tLRAT (15 μM) in a buffer containing 50 mM sodium phosphate, pH 7.4, 100 mM NaCl, and 10 mM DTT is shown as absorbance vs radial position at equilibrium at 20 °C and 45 000 rpm. The scans were taken at 280 nm and 0.01 mm radial step resolution. Analysis of the scanned data was performed with the Origin 3.78 program. The raw data (circles) and the global fit of a monomer−dimer equilibrium model (lines) are shown.

The liver also has an extensive smooth endoplasmic reticulum, consistent with the staining pattern. Intense staining of the hepatocytes is also consistent with the well-known ability of these cells to process retinol into retinyl esters and store the retinoid in this form (*25*). Control sections of liver, which are negative, are shown in Figure 8c.

DISCUSSION

LRAT is the only member of a novel class of recently discovered proteins whose function is known (*4*, *17*). Included in this family of proteins are tumor suppressors and putative viral proteases, making this group of proteins of substantial interest. Consequently, it is of interest to understand the molecular basis of LRAT action and eventually to determine its structure as a founder member of a new series of proteins. As mentioned previously, LRAT is a membrane bound enzyme and contains at least two transmembrane segments at its N- and C-termini (*4*). While LRAT has been partially purified, the complete purification of the protein from biological sources has not met with success. In common with many membrane bound proteins, as purification of the detergent solubilized enzyme proceeds, the activity sharply diminishes. Full-length LRAT has already been cloned and expressed in HEK cells, but here again there is no method available for purification of this protein, which is contaminated by all of the other proteins resident in HEK membranes. In addition, the level of expression of LRAT in these membranes is quite limited (*4*). The current studies address the goal of preparing a modified version of LRAT to produce substantial quantities of purified enzyme needed for functional, structural, and mechanistic studies.

Simple hydropathy plots of LRAT suggest that the N- and C-terminal regions are transmembrane segments (*4*). In the current studies, the N- and C-terminal segments were deleted, giving rise to a truncated version of LRAT, referred to as tLRAT. Since none of the known catalytically important residues (*15*, *16*) are present in these two terminal regions, it was anticipated that the tLRAT would still maintain catalytic activity and thus serve as a starting point for further studies on LRAT function. In addition to having truncated

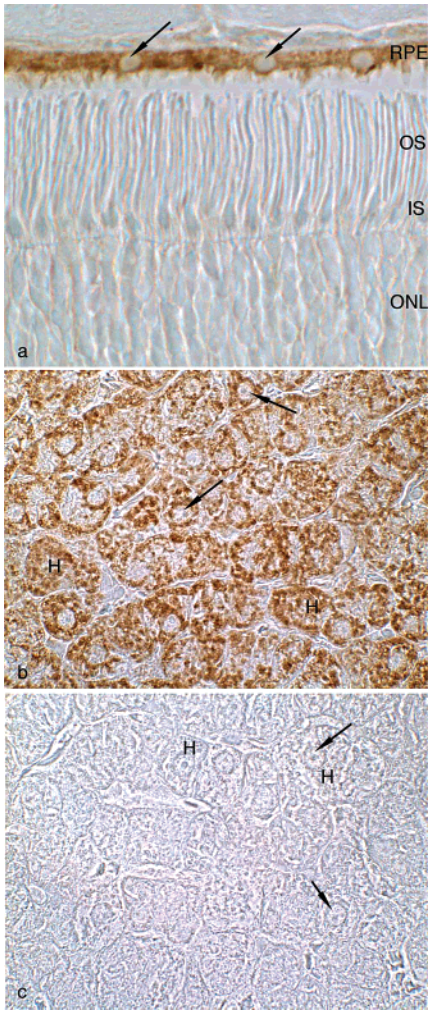

FIGURE 8: Immunocytochemistry of bovine retina and liver using affinity purified anti tLRAT antibodies. (a) In the retina, staining is limited to the retinal pigment epithelium (RPE). Retinal photoreceptor outer segments (OS), inner segments (IS), and outer nuclear layer (ONL) are shown for comparison. (b) Staining in the liver is observed in hepatocytes (H). The nuclei of the RPE and hepatocytes (arrows) are negative, consistent with the putative location of LRAT in the smooth endoplasmic reticulum of cells. (c) Control section of liver in which immune IgG was replaced with preimmune IgG. × 270.

N- and C-terminal regions, tLRAT also contains a His-tag at its C-terminus, facilitating its purification. We have previously described the use of human LRAT (hLRAT), encoding constructs containing the wild-type nucleotide sequence (*4*). These constructs have been used for the evaluation of LRAT protein expression and enzymatic activity following induction in eukaryotic cells (*4*). In the current study, an expression vector pET 21b(+) was used for the generation of two constructs. The first one contained a 690 bp DNA fragment encoding a polypeptide of 230 amino acid residues, which represented the entire coding sequence of hLRAT (*4*). In the second construct, a DNA fragment of 495 bp encoding only the intracellular loop of the putative LRAT structure was generated (*20*). The intent was to remove the two transmembrane domains from the amino and carboxy terminals of hLRAT polypeptide to increase solubility and further characterize enzymatic activity. We also wanted to produce a form of LRAT that might be useful for kinetic analysis, structural analysis, and generation of antibodies since only anti-LRAT peptide antibodies are available at this time (*4*).

In bacteria, tLRAT can be expressed in high yield. The tLRAT produced in bacteria, however, is not immediately extracted by mere disruption and centrifugation. Under these conditions, most of the tLRAT sediments during centrifugation, suggesting that the protein is either in inclusion bodies or forms aggregates. Therefore, detergents were used to extract tLRAT from bacteria. Simple detergents, such as guanidinium hydrochloride and urea, while capable of solubilizing tLRAT, led to a tLRAT protein that was catalytically inert and not readily activated. The most effective detergent with respect to yield of extraction was 1% SDS. Using 1% SDS, the tLRAT could essentially be quantitatively extracted from the bacteria. Unfortunately, the enzyme is completely inert in 1% SDS. However, substantial activity can be regained either by diluting the SDS to 0.05% or by removing some of the SDS by precipitation to lower its overall concentration. Under these conditions, substantial catalytic activity is regained. Detergents milder than SDS were also sought to extract and purify tLRAT. The milder detergents, including CHAPSO and Triton-X, while not as effective in solubilizing tLRAT from bacteria as 1% SDS, produced a form of tLRAT that retains the highest enzymatic activity without further manipulation. tLRAT extracted in this manner might be preferred both for structural and mechanistic studies in the future.

tLRAT, produced in milligram quantities by affinity chromatography, provided an excellent antigen for the production of antibodies directed against a substantial portion of the protein mass. This is significant since the only antibodies currently available are directed against LRAT peptides (*4*). The anti tLRAT antibodies are robust in their identification of tLRAT and LRAT by Western blot analysis and provided excellent reagents for future immunocytochemical localization of LRAT in diverse tissues. Localization of LRAT with these antibodies in the pigment epithelium of the retina and in the liver are consistent with our current understanding that this protein resides in the endoplasmic reticulum (ER). From electron microscopic evidence, it is known that both the RPE and liver have an abundance of ER membranes distributed throughout the cytoplasm. The general distribution of the staining reaction in the RPE (Figure 8a) and hepatocytes (Figure 8b) with exclusion from the nucleus is in accord with this.

The availability of purified tLRAT enables us to begin a variety of experiments to probe the structure and function of this novel enzyme. First, the fact that tLRAT retains enzymatic activity clearly indicates that the N- and C-terminal regions of the protein are not essential for catalysis. This is consistent with what is already known from site-specific mutagenic experiments (*15*, *16*). Having pure tLRAT allows for an exploration of its substrate specificity with respect to the physiologically relevant retinols (*12*). It is well-known that both all-*trans*- and 11-*cis*-retinyl esters are components of the visual cycle (*2*, *3*, *7*). Consequently, it was of some interest to determine whether purified tLRAT could esterify both all-*trans*- and 11-*cis*-retinols. In a current model for the visual cycle function, all-*trans*-retinyl esters are the actual substrates for isomerization to 11-*cis*-retinoids, and so the LRAT esterification of all-*trans*-retinol plays an important role in the visual cycle (*2*, *7*, *8*). In the case of

11-*cis*-retinyl esters, the role of 11-*cis*-retinol acylation lies in the storage of excess 11-*cis*-retinol in the stable retinyl ester form. Kinetic studies on tLRAT demonstrated that both all-*trans*-retinol and 11-*cis*-retinol are substrates for tLRAT. This means, of course, that there need not be a separate LRAT enzyme in RPE membranes to esterify both 11-*cis*-retinol and all-*trans*-retinol. It is noteworthy though that tLRAT is a more effective catalyst (approximately 10-fold) for acylating all-*trans*-retinol than it is for 11-*cis*-retinol. This is understandable in terms of the relative roles of all-*trans*-retinyl esters versus 11-*cis*-retinyl esters. LRAT has a much more dynamic role to play in the all-*trans*-retinyl ester biosynthesis inasmuch as these molecules are critical substrates along the isomerization pathway (*2*, *7*, *8*). The formation of 11-*cis*-retinyl esters is presumably of less physiologic consequence because these molecules are simply convenient storage forms. It is interesting to note that all-*trans*-retinyl esters dominate in the all-*trans*-retinoid series, while the same is not true in the 11-*cis*-retinoid series where significant steady-state levels of 11-*cis*-retino(a)l are found in the RPE (*26*).

The experiments on tLRAT specificity were also mirrored by experiments using cloned full-length LRAT from HEK cells (*4*). Here, of course, the enzyme could not be purified, but inasmuch as HEK cells do not themselves significantly process retinoids, it is possible to investigate whether full-length LRAT can process both all-*trans*- and 11-*cis*-retinol. In fact, full-length LRAT expressed in HEK cells also can process both all-*trans*-retinol and 11-*cis*-retinol and is a substantially more powerful catalyst for all-*trans*-retinol as substrate. Therefore, at least by these modest structure activity studies, the tLRAT behaves similarly to full-length LRAT.

Cross-linking and other biochemical studies in RPE membranes have already shown that LRAT behaves as a functional dimer (*22*). It was of interest to see if oligomerization of tLRAT also occurs. In fact, tLRAT readily forms dimers as evidenced by nondenaturing gel electrophoresis, and a substantial amount of dimer is revealed by analytic ultracentrifugation. Therefore, dimer formation is inherent in this member of the LRAT family and does not require the N- and C-terminal hydrophobic regions to express this capability. The protein−protein interactions that drive this dimerization may reside in hydrophobic surfaces of LRAT beyond the N- and C-termini. Indeed, one hydropathy plot representation for LRAT suggests that it may possess four rather than two transmembrane domains (*4*, *17*). Even if the nonterminal hydrophobic domains of LRAT are not transmembrane, they might form hydrophobic protein−protein contacts that could promote dimer formation. While dimeric LRAT has been shown to be fully catalytically active (*22*), it is not currently known whether each homodimer expresses two active sites or one.

The current studies demonstrate that catalytically tLRAT can be readily expressed and purified from bacteria. Despite the loss of the N- and C-termini of LRAT, tLRAT behaves similarly to LRAT both with respect to retinol substrate specificity and propensity to form dimers. The availability of pure LRAT will enable the performance of mechanistic and structural studies on an unusual class of enzymes of which LRAT is the founder member.

ACKNOWLEDGMENT

The authors thank Teresita Yang and Marcia Lloyd for their expert technical assistance in the preparation of the tissue sections and immunocytochemistry of LRAT, respectively. The technical assistance of Dr. Sunghyouk Park for the sedimentation equilibrium analysis is greatly acknowledged.

SUPPORTING INFORMATION AVAILABLE

Experiments on the kinetics, synthesis of ^{3}H-11-*cis*-retinol, and mass spectroscopic analysis. This material is available free of charge via the Internet at http://pubs.acs.org.

REFERENCES

1. MacDonald, P. N., and Ong, D. E. (1988) *J. Biol. Chem. 263*, 12478−12482.
2. Barry, R., Cañada, F. J., and Rando, R. R. (1989) *J. Biol. Chem. 264*, 9231−9238.
3. Saari, J. C., and Bredberg, D. L. (1989) *J. Biol. Chem. 264*, 8636−8640.
4. Ruiz, A., Winston, A., Lim, Y.-H., Gilbert, B. Z., Rando, R. R., and Bok, D. (1999) *J. Biol. Chem. 274*, 3834−3841.
5. MacDonald, P. N., and Ong, D. E. (1988) *Biochem. Biophys. Res. Commun. 156*, 157−163.
6. Fong, S. L., Bridges, C. D., and Alvarez, R. A. (1983) *Vision Res. 23*, 47−52.
7. Bernstein, P. S., Law, W. C., and Rando, R. R. (1987) *Proc. Natl. Acad. Sci. U.S.A. 84*, 1849−1853.
8. Deigner, P. S., Law, W. C., Cañada, F. J., and Rando, R. R. (1989) *Science 244*, 968−971.
9. Moiseyev, G., Crouch, R. K., Goletz, P., Oatis, J., Redmond, T. M., Ma, J.-x. (2003) *Biochemistry 42*, 2229−2238.
10. Gollapolli, D., and Rando, R. R. (2003) *Biochemistry*, in press.
11. Fulton, B. S., and Rando, R. R. (1987) *Biochemistry 26*, 7938−7945.
12. Cañada, F. J., Law, W. C., Rando, R. R., Yamamoto, T., Deguini, F., and Nakanishi, K. (1990) *Biochemistry 29*, 9690−9697.
13. Shi, Y.-Q., Hubacek, I., and Rando, R. R. (1993) *Biochemistry 32*, 1257−1263.
14. Shi, Y. Q., Furuyoshi, S., Hubacek, I., and Rando, R. R. (1993) *Biochemistry 32*, 3077−3080.
15. Mondal, M. S., Ruiz, A., Bok, D., and Rando, R. R. (2000) *Biochemistry 39*, 5215−5220.
16. Mondal, M. S., Ruiz, A., Hu, J., Bok, D., and Rando, R. R. (2001) *FEBS Lett. 489*, 14−18.
17. Rando, R. R. (2001) *Chem. Rev. 101*, 1881−1896.
18. Hughes, P. J., and Stanway, G. (2000) *J. Gen. Virol. 81*, 201−207.
19. Laemmli, U. K. (1970) *Nature 227*, 680−685.
20. Ruiz, A., Kuehn, M. H., Andorf, J. L., Stone, E., Hageman, G. S., and Bok, D. (2001) *Invest. Ophthalmol. Vis. Sci. 42*, 31−37.
21. Sambrook, J., Fritsch, E. F., and Maniatis, T. (1989) *Molecular Cloning*, 2nd ed., Vols. I−III, Cold Spring Harbor, Laboratory Press.
22. Jahng, W. J., Cheung, E., and Rando, R. R. (2002) *Biochemistry 41*, 6311−6319.
23. Begg, G. E., Harper, S. L., Morris, M. B., and Speicher, D. W. (2000) *J. Biol. Chem. 275*, 3276−3287.
24. Myers, D. P., Jackson, L. K., Ipe, V. G., Murphy, G. E., and Phillips, M. A. (2001) *Biochemistry 40*, 13230−13236.
25. Zolfaghari, R., and Ross, A. C. (2002) *J. Nutr. 132*, 1160−1164.
26. Saari, J. C. (2000) *Invest. Ophth. Vis. Sci. 41*, 337−348.

BI0342416